Averaged Models of Multiphase Flows

In collaboration with C. Caia and K. Nandakumar

University of Alberta, Canada

CONTENTS

- Introduction.
- Comparison of various models.
- Discretization procedure.
- Simulation of void fraction waves.
- Bubble column reactors.
- Conclusions

INTRODUCTION

- Interpenetrating continua.
- Averaged models.
- Closure relations.
- Qualitative comparison of various models.
- Numerical methods for advection dominated problems.
- Validation problems.

TWO-PHASE MODELS

$$\frac{\partial \Phi}{\partial t} + \nabla \cdot (\Phi \mathbf{v}) = \mathbf{0} \tag{1}$$

$$\frac{\partial (1-\Phi)}{\partial t} + \nabla \cdot ((1-\Phi)\mathbf{u}) = \mathbf{0} \tag{2}$$

$$\Phi \rho_2 \frac{D_{\mathbf{v}}\mathbf{v}}{\mathbf{Dt}} = -\Phi \nabla p - \xi(\Phi)\nabla\Phi - \beta(\Phi)(\mathbf{v}-\mathbf{u}) - \Phi\rho_{\mathbf{2}}\mathbf{g} -$$

$$\Phi \rho_1 \mu(\Phi) \frac{D_{\mathbf{v}}(\mathbf{v}-\mathbf{u})}{\mathbf{Dt}} + \nabla \cdot (\mu_d(\Phi)\nabla\mathbf{v}) \tag{3}$$

$$(1-\Phi)\rho_1 \frac{D_{\mathbf{u}}\mathbf{u}}{\mathbf{Dt}} = -(1-\Phi)\nabla p + \xi(\Phi)\nabla\Phi + \beta(\Phi)(\mathbf{v}-\mathbf{u}) -$$

$$(1-\Phi)\rho_1\mathbf{g} + \Phi\rho_1\mu(\Phi)\frac{D_{\mathbf{v}}(\mathbf{v}-\mathbf{u})}{Dt} + \nabla \cdot (\mu_c \nabla \mathbf{u}) \tag{4}$$

TWO-PHASE MODELS

$$A_1(\phi)\frac{\partial v}{\partial t} + A_2(\phi)\frac{\partial u}{\partial t} + B_1(\phi)v\frac{\partial v}{\partial x} + B_2(\phi)u\frac{\partial u}{\partial x} + B_3(\phi)u\frac{\partial v}{\partial x} + B_4(\phi)v\frac{\partial u}{\partial x} = -\beta(\phi, |v-u|)(v-u) - \xi(\phi)\frac{\partial \phi}{\partial x} + \phi(\rho_1 - \rho_2)g + \frac{\partial}{\partial x}\left(\mu_d(\phi)\frac{\partial v}{\partial x}\right) \quad (5)$$

$$\frac{\partial \phi}{\partial t} + \frac{\partial(\phi v)}{\partial x} = 0 \quad (6)$$

$$\frac{\partial(1-\phi)}{\partial t} + \frac{\partial[(1-\phi)u]}{\partial x} = 0 \quad (7)$$

where $A_1 = B_1 > 0, A_2 < 0$
Solution: $\phi = \phi_0$, $u = 0$, $v = v_0 = \phi_0(\rho_1 - \rho_2)g/\beta(\phi_0)$.

LINEAR ANALYSIS

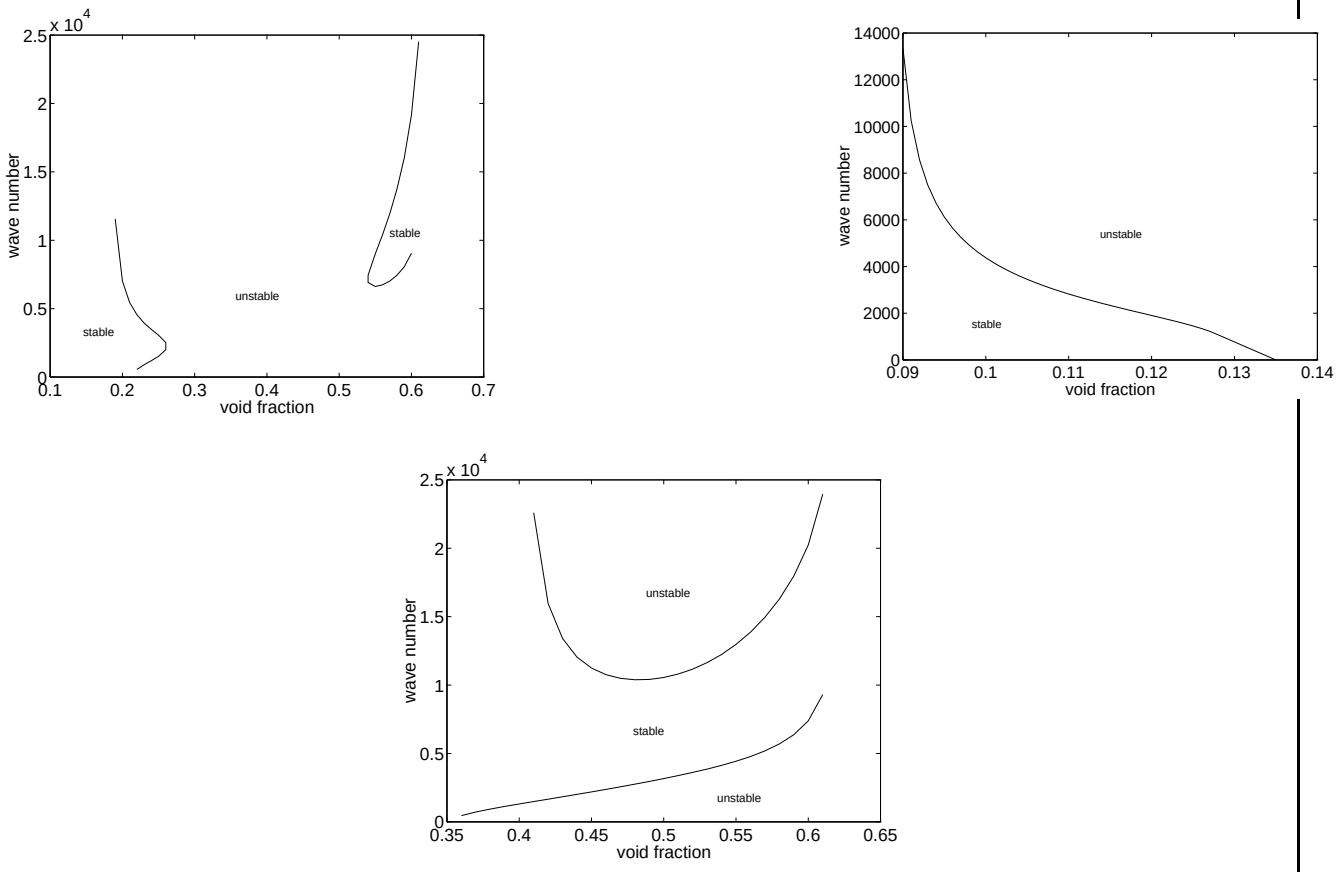

Figure 1: Neutral stability curves.

LINEAR ANALYSIS (cont.)

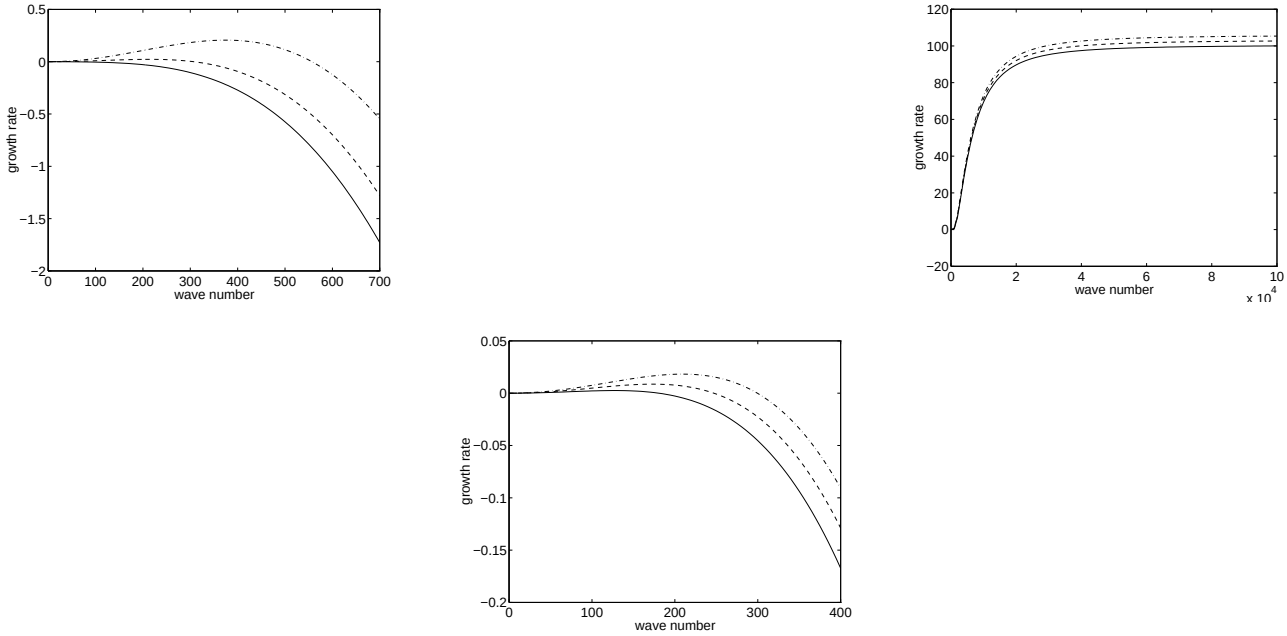

Figure 2: Growth rate vs. k: case (i) (first row, left;- $\phi = 0.212$, – $\phi = 0.215$, -. $\phi = 0.22$); case (iii) (first row, right; - $\phi = 0.13$, – $\phi = 0.131$, -. $\phi = 0.132$); and case (v) (second row; left;- $\phi = 0.353$, – $\phi = 0.354$, -. $\phi = 0.355$).

Weakly non-linear analysis

$$\tau = \epsilon^3 t, \quad \eta = \epsilon(x - c_0 t) \tag{8}$$

$$\begin{aligned} u &= u_2\epsilon^2 + u_3\epsilon^3 + ... \\ v &= v_0 + v_2\epsilon^2 + v_3\epsilon^3 + ... \\ \phi &= \phi_0 + \phi_2\epsilon^2 + \phi_3\epsilon^3 + ... \end{aligned} \tag{9}$$

$$\frac{\partial \phi_2}{\partial \tau} + \lambda_0 \frac{\partial \phi_2^2}{\partial \eta} + \gamma_0 \frac{\partial^3 \phi_2}{\partial \eta^3} = 0 \tag{10}$$

$$\phi_2(\eta) = \frac{6\gamma_0}{\lambda_0} k^2 \mathrm{sech}^2[k(\eta - \eta_0 - 4\gamma_0 k^2 \tau)] \tag{11}$$

$$\frac{\partial \phi_3}{\partial \tau} + 2\lambda_0 \frac{\partial \phi_2 \phi_3}{\partial \eta} + \gamma_0 \frac{\partial^3 \phi_3}{\partial \eta^3} = -\frac{\partial^2 \phi_2}{\partial \eta^2} - \lambda_0' \frac{\partial^2 \phi_2^2}{\partial \eta^2} - \gamma_0' \frac{\partial^4 \phi_2}{\partial \eta^4} \tag{12}$$

$$\frac{\partial \phi_4}{\partial \tau} + 2\lambda_0 \frac{\partial \phi_2 \phi_4}{\partial \eta} + \gamma_0 \frac{\partial^3 \phi_4}{\partial \eta^3} = f(\phi_2, \phi_3, \frac{\partial \phi_2}{\partial \eta}, \frac{\partial \phi_3}{\partial \eta}, ..., \frac{\partial^5 \phi_2}{\partial \eta^5}) \tag{13}$$

Weakly non-linear analysis (cont.)

$$\theta = k(\eta - \eta_0 - 4\gamma_0 k^2 \tau), \quad s = \tau \tag{14}$$

$$\begin{gathered} -4\phi_3 + 12\text{sech}^2\theta\phi_3 + \frac{\partial^2\phi_3}{\partial\theta^2} = \\ \frac{12k}{\lambda_0}(\text{tanh}\theta\text{sech}^2\theta + 2\lambda_0'\text{tanh}\theta\text{sech}^4\theta \\ +4k^2\gamma_0'\text{tanh}\theta\text{sech}^2\theta - 12k^2\gamma_0'\text{tanh}\theta\text{sech}^4\theta) + A = R(\theta) \end{gathered} \tag{15}$$

Particular solution: $w = \text{sech}^2\theta\text{tanh}\theta$
General solution: $\phi_3 = wv$

$$v = B + C\int \frac{d\theta}{w(\theta)} + \int \frac{d\theta}{w(\theta)^2}\int w(\theta)R(\theta)d\theta \tag{16}$$

Boundedness of ϕ_3 requires:

$$C = 0, \quad 8\lambda_0' - 20\gamma_0' k^2 + 7 = 0 \tag{17}$$

Weakly non-linear analysis (cont.)

$$\phi_3(\theta) = \frac{A}{16} - \frac{3A}{16}\tanh^2\theta + \frac{9A}{16}\mathrm{sech}^2\theta + (B - \frac{A}{2})\tanh\theta\mathrm{sech}^2\theta$$
$$+\frac{1}{4\lambda_0}(-3A\lambda_0 - 12k - \frac{192}{7}\lambda_0' k + \frac{816}{7}\gamma_0' k^3)\theta\tanh\theta\mathrm{sech}^2\theta \quad (18)$$
$$+\frac{1}{4\lambda_0}(\frac{96}{7}\lambda_0' k - \frac{576}{7}\gamma_0' k^3)\ln(e^{2\theta}+1)\tanh\theta\mathrm{sech}^2\theta$$

Since $\phi_3 \to 0$ as $\theta \to \infty$ then $A = 0$.

TWO-PHASE FLOW MODELING

- Governing equations in the non-dimensional form are: (1),(2) and

$$\alpha\Phi\frac{D_{\mathbf{v}}\mathbf{v}}{Dt} = -\Phi\nabla p - \frac{\alpha\xi(\Phi)}{\rho_2 v_\star^2}\nabla\Phi - \frac{1}{Fr}\frac{\Phi(1-\Phi)^2}{\bar{U}(\Phi)}(\mathbf{v}-\mathbf{u}) -$$

$$\frac{\alpha}{Fr}\frac{\Phi}{1-\alpha}(0,0,1) - \Phi\mu(\Phi)\frac{D_{\mathbf{v}}(\mathbf{v}-\mathbf{u})}{Dt} + \frac{\alpha}{\rho_2 l v_\star}\nabla\cdot(\mu_d(\Phi)\nabla\mathbf{v}) \quad (19)$$

$$(1-\Phi)\frac{D_{\mathbf{u}}\mathbf{u}}{\mathbf{Dt}} = -(1-\Phi)\nabla p + \frac{\xi(\Phi)}{\rho_1 v_\star^2}\nabla\Phi + \frac{1}{Fr}\frac{\Phi(1-\Phi)^2}{\bar{U}(\Phi)}(\mathbf{v}-\mathbf{u}) -$$

$$\frac{1}{Fr}\frac{1-\Phi}{1-\alpha}(0,0,1) + \Phi\mu(\Phi)\frac{D_{\mathbf{v}}(\mathbf{v}-\mathbf{u})}{\mathbf{Dt}} + \frac{1}{\rho_1 l v_\star}\nabla\cdot(\mu_c\nabla\mathbf{u}) \quad (20)$$

$$\alpha = \frac{\rho_2}{\rho_1} \quad \text{(density ratio)} \quad Fr = \frac{\rho_1}{\rho_1-\rho_2}\frac{v_\star^2}{gl} \quad \text{(Froude number)}$$

TWO-PHASE FLOW MODELING(cont.)

The material (total) derivatives $\frac{D_{\mathbf{v}}}{Dt}$ and $\frac{D_{\mathbf{u}}}{Dt}$ stand for:

$$\frac{D_{\mathbf{v}}\mathbf{w}}{\mathbf{Dt}} := \frac{\partial \mathbf{w}}{\partial \mathbf{t}} + \mathbf{v} \cdot \nabla \mathbf{w}$$

$$\frac{D_{\mathbf{u}}\mathbf{w}}{\mathbf{Dt}} := \frac{\partial \mathbf{w}}{\partial \mathbf{t}} + \mathbf{u} \cdot \nabla \mathbf{w}$$

The expressions of the coefficients are:

$$\mu(\Phi) = \frac{1}{2}\frac{1+2\Phi}{1-\Phi}$$

$$\beta(\Phi) = \frac{\Phi(1-\Phi)^2(\rho_1-\rho_2)g}{U(\Phi)}$$

$$U(\Phi) = v_\infty(1-\Phi)(1-\Phi+0.55\Phi^2)$$

$$v_\infty = 0.219\, m/s$$

$$\frac{\xi(\Phi)}{(1-\Phi)\rho_1 v_\star^2} = \frac{(v-\overline{U}_m)^2\Phi}{(1-\Phi)^3} + \frac{\bar{D}}{\overline{\overline{U}}(\Phi)} -$$

$$(\overline{U}_m + \overline{U}(\Phi) + \alpha_2(\Phi)\overline{U}(\Phi) - \bar{a}(\Phi)\alpha_1(\Phi))\frac{d\overline{U}}{d\Phi}$$

where

$$U_m = \Phi v + (1-\Phi)u$$

TWO-PHASE FLOW MODELING(cont.)

$$a(\Phi) = U_m + v_\infty(1-\Phi)(1-3.08\Phi+2.77\Phi^2-0.55\Phi^3)$$

$a(\Phi)$ represents the kinematic wave speed and was chosen by Lammers *et al.* (1996) to be in agreement with their experiments.
Performing a weakly nonlinear analysis, we ended up with the generalized Burgers' equation:

$$\frac{\partial \Phi_1}{\partial x} + (\frac{1}{\bar{a}_0} - \frac{\bar{a}_1}{\bar{a}_0^2}\Phi_1)\frac{\partial \Phi_1}{\partial t} = \frac{\bar{D}}{\bar{a}_0^3}\frac{\partial^2 \Phi_1}{\partial t^2}$$

D represents the effective diffusivity measured in the experiments and was always found to be positive.This yields to the Generalized Burgers equation with a positive viscosity whose solutions are expected to be stable.

TWO-PHASE FLOW MODELING(cont.)

- Discretization scheme

  Operator splitting :

$$\Phi^{n+1}\frac{3\mathbf{v}^{n+1}-4\tilde{\mathbf{v}}^{n}+\tilde{\mathbf{v}}^{n-1}}{2\Delta t}=-\frac{1}{\alpha}\Phi^{n+1}\nabla p^{n+1}+$$

$$f_1(\mathbf{u}^{n+1},\mathbf{v}^{n+1},\Phi^{n+1})-\frac{1}{\alpha}\Phi^{n+1}\mu(\Phi^{n+1})$$

$$\left(\frac{3\mathbf{v}^{n+1}-4\tilde{\mathbf{v}}^{n}+\tilde{\mathbf{v}}^{n-1}}{2\Delta t}-\frac{3\mathbf{u}^{n+1}-4\tilde{\mathbf{u}}^{n}+\tilde{\mathbf{u}}^{n-1}}{2\Delta t}\right)+$$

$$\frac{1}{\rho_2 l v^{\star}}\nabla\cdot(\mu_d(\Phi)\nabla\mathbf{v}^{n+1}) \tag{21}$$

$$(1-\Phi^{n+1})\frac{3\mathbf{u}^{n+1}-4\tilde{\mathbf{u}}^{n}+\tilde{\mathbf{u}}^{n-1}}{2\Delta t}=-(1-\Phi^{n+1})\nabla p^{n+1}+$$

$$f_2(\mathbf{u}^{n+1},\mathbf{v}^{n+1},\Phi^{n+1})+\Phi^{n+1}\mu(\Phi^{n+1})$$

$$\left(\frac{3\mathbf{v}^{n+1}-4\tilde{\mathbf{v}}^{n}+\tilde{\mathbf{v}}^{n-1}}{2\Delta t}-\frac{3\mathbf{u}^{n+1}-4\tilde{\mathbf{u}}^{n}+\tilde{\mathbf{u}}^{n-1}}{2\Delta t}\right)$$

$$\frac{1}{\rho_1 l v^{\star}}\nabla\cdot(\mu_c\nabla\mathbf{u}^{n+1}) \tag{22}$$

TWO-PHASE FLOW MODELING(cont.)

where $\tilde{\mathbf{u}}^{n-i}(i=0,1)$ and $\tilde{\mathbf{v}}^{n-i}(i=0,1)$ are the "advected" velocity fields at time level n+1 and are found by solving the initial-value problems:

$$\begin{aligned}\frac{\partial \tilde{\mathbf{u}}^{n-i}(s)}{\partial s} &= -(\tilde{\mathbf{u}}^{n-i}(s)\cdot\nabla)\tilde{\mathbf{u}}^{n-i}(s),\\ 0 \le s \le (i+1)\Delta t, &\quad i=0,1\\ \tilde{\mathbf{u}}^{n-i}(0) &= \mathbf{u}^{n-i}\end{aligned} \tag{23}$$

and

$$\begin{aligned}\frac{\partial \tilde{\mathbf{v}}^{n-i}(s)}{\partial s} &= -(\tilde{\mathbf{v}}^{n-i}(s)\cdot\nabla)\tilde{\mathbf{v}}^{n-i}(s),\\ 0 \le s \le (i+1)\Delta t, &\quad i=0,1\\ \tilde{\mathbf{v}}^{n-i}(0) &= \mathbf{v}^{n-i}\end{aligned} \tag{24}$$

$$\tilde{\mathbf{u}}(t^{n+1}) = \tilde{\mathbf{u}}^n, \quad \tilde{\mathbf{v}}(t^{n+1}) = \tilde{\mathbf{v}}^n$$

Method of characteristic for $\tilde{\mathbf{u}}^n$, $\tilde{\mathbf{v}}^n$, Φ^{n+1}.

TWO-PHASE FLOW MODELING(cont.)

- Characteristic equations

$$\frac{d\mathbf{X}_{\mathbf{x}}^{n+1}(t)}{dt} = \mathbf{u}(\mathbf{X}_{\mathbf{x}}^{n+1}(t), t), \quad \text{in} \quad [t^{n-i}, t^{n+1}[$$
$$\mathbf{X}_{\mathbf{x}}^{n+1}(t^{n+1}) = \mathbf{x}$$

- The convected velocity fields are given by:

$$\tilde{\mathbf{u}}^{n-i}(\mathbf{x}) = \mathbf{u}^{n-i}(\mathbf{X}_{\mathbf{x}}^{n+1}(t^{n-i})), \quad i = 0, 1$$

1. Second order extrapolation of the velocity field to time level t^{n+1}, $\mathbf{u}_e^{n+1}$:

$$\mathbf{u}_e^{n+1} = 2\mathbf{u}^n - \mathbf{u}^{n-1}$$

2. Solve the characteristic equation

$$\mathbf{X}_{\mathbf{x}}^{n+1}(t^{n-i}) = \mathbf{X}_{\mathbf{x}}^{n+1}(t^{n+1}) - i\Delta t\mathbf{u}_e^{n+1} \quad i = 0, 1$$

3. Determine which elements contain the feet of the characteristics $\mathbf{X}_{\mathbf{x}}^{n+1}(t^{n-i})$.

4. Interpolate velocity field at time $t^{n-i}, i = 0, 1$ onto the feet of the characteristics $\mathbf{X}_{\mathbf{x}}^{n-i}$ using the finite element interpolant based on the Eulerian grid.

TWO-PHASE FLOW MODELING(cont.)

The momentum equations for the intermediate velocities $\mathbf{u}^\star$ and $\mathbf{v}^\star$ are:

$$\Phi^{n+1}\frac{3\mathbf{v}^\star - \mathbf{4\tilde{v}^n} + \mathbf{\tilde{v}^{n-1}}}{2\Delta t} = -\frac{1}{\alpha}\Phi^{n+1}\nabla p^n +$$

$$f_1(\mathbf{u}^\star, \mathbf{v}^\star, \Phi^{\mathbf{n+1}}) - \frac{\mathbf{1}}{\alpha}\Phi^{\mathbf{n+1}}\mu(\Phi^{\mathbf{n+1}}))$$

$$\left(\frac{3\mathbf{v}^\star - 4\tilde{\mathbf{v}}^n + \tilde{\mathbf{v}}^{n-1}}{2\Delta t} - \frac{3\mathbf{u}^\star - 4\tilde{\mathbf{u}}^n + \tilde{\mathbf{u}}^{n-1}}{2\Delta t}\right) +$$

$$\frac{1}{\rho_2 l \mathbf{v}^\star}\nabla\cdot(\mu_d(\Phi)\nabla\mathbf{v}^\star) \tag{25}$$

$$(1-\Phi^{n+1})\frac{3\mathbf{u}^\star - 4\tilde{\mathbf{u}}^n + \tilde{\mathbf{u}}^{n-1}}{2\Delta t} = -(1-\Phi^{n+1})\nabla p^n +$$

$$f_2(\mathbf{u}^\star, \mathbf{v}^\star, \Phi^{n+1}) +$$

$$\Phi^{n+1}\mu(\Phi^{n+1})\left(\frac{3\mathbf{v}^\star - 4\tilde{\mathbf{v}}^n + \tilde{\mathbf{v}}^{n-1}}{2\Delta t} - \frac{3\mathbf{u}^\star - 4\tilde{\mathbf{u}}^n + \tilde{\mathbf{u}}^{n-1}}{2\Delta t}\right) +$$

$$\frac{1}{\rho_1 l \mathbf{v}^\star}\nabla\cdot(\mu_c\nabla\mathbf{u}^\star) \tag{26}$$

$$\Phi^{n+1}\frac{3}{2}\left(\frac{\mathbf{v}^{n+1}-\mathbf{v}^{\star}}{\Delta t}\right)=-\frac{1}{\alpha}\Phi^{n+1}(\nabla p^{n+1}-\nabla p^{n})$$

$$-\frac{1}{\alpha}\Phi^{n+1}\mu(\Phi^{n+1})\frac{3}{2}\left(\frac{\mathbf{v}^{n+1}-\mathbf{v}^{\star}}{\Delta t}-\frac{\mathbf{u}^{n+1}-\mathbf{u}^{\star}}{\Delta t}\right) \tag{27}$$

and

$$(1-\Phi^{n+1})\frac{3}{2}\left(\frac{\mathbf{u}^{n+1}-\mathbf{u}^{\star}}{\Delta t}\right)=-(1-\Phi^{n+1})(\nabla p^{n+1}-\nabla p^{n})$$

$$+\Phi^{n+1}\mu(\Phi^{n+1})\frac{3}{2}\left(\frac{\mathbf{v}^{n+1}-\mathbf{v}^{\star}}{\Delta t}-\frac{\mathbf{u}^{n+1}-\mathbf{u}^{\star}}{\Delta t}\right) \tag{28}$$

$$\nabla\cdot(\rho_2\Phi\mathbf{v}+\rho_1(1-\Phi)\mathbf{u})=(\rho_1-\rho_2)\frac{\partial\Phi}{\partial t} \tag{29}$$

$$\frac{3}{2}(\rho_1-\rho_2)\left(\frac{3\Phi^{n+1}-4\Phi^{n}+\Phi^{n-1}}{2\Delta t}\right)=$$

$$\frac{3}{2}\nabla\cdot(\Phi^{n+1}\rho_2\mathbf{v}^{\star}+(1-\Phi^{n+1})\rho_1\mathbf{u}^{\star})-\Delta t\nabla\cdot(\nabla p^{n+1}-\nabla p^{n}) \tag{30}$$

TWO-PHASE FLOW MODELING(cont.)

Let us consider two nested grids of sizes H and h, where $H = 2h$, which generate corresponding finite element functional spaces denoted by $(\mathbf{X}_H)$ and $(\mathbf{X}_h)$. The basis for the difference space $\mathbf{X}_h^H$, based on the decomposition $\mathbf{X}_h = \mathbf{X}_H \oplus \mathbf{X}_h^H$, is given by:

$$(\varphi_h^H)_i = \begin{cases} \varphi_{h,i}\,, & \text{if } i \in \tau_h - \tau_H \\ \varphi_{h,i} - \varphi_{H,i}\,, & \text{if } i \in \tau_H \end{cases} \tag{31}$$

For an easy implementation, $\mathbf{X}_H$ is injected into $\mathbf{X}_h$, using the representation of the basis functions:

$$\varphi_H^k = \sum_{j=1}^{35} a_j^k \varphi_h^j$$

In order to find a_j^k, we solve the following systems

$$\langle \varphi_H^k, \varphi_h^i \rangle = \sum_{j=1}^{35} a_j^k \langle \varphi_h^j, \varphi_h^i \rangle \quad i,j = 1,...,35, \quad k = 1,...,10$$

TWO-PHASE FLOW MODELING(cont.)

Weak formulation:

Find $\mathbf{u}_h \in \mathbf{X}_h$ s.t. $a(\mathbf{u}_h, \mathbf{V}_h) + b_h(\mathbf{u}_h^H, \mathbf{v}_h^H) = (\mathbf{f}, \mathbf{v}_h), \quad \forall \mathbf{v}_h \in \mathbf{X}_h$

$$b_h(\mathbf{u}_h^H, \mathbf{v}_h^H) = c_b \sum_{\mathbf{K}_h \in \tau_h} \text{meas}(\mathbf{K}_h)^{1/3} \int_{\mathbf{K}_h} (\nabla \mathbf{u}_h^H \cdot \nabla \mathbf{v}_h^H).$$

$$c_h(\mathbf{u}_h^H, \mathbf{v}_h, \mathbf{w}_h) = c_{sc} \sum_{\mathbf{K}_H \in \tau_H} \text{meas}(\mathbf{K}_H)^{1/3} \frac{||\nabla \mathbf{u}_h^H||_{0,\mathbf{K}_H}}{||\nabla \mathbf{u}_h||_{0,\mathbf{K}_H}} \int_{\mathbf{K}_H} (\nabla \mathbf{v}_h \cdot \nabla \mathbf{w}_h)$$

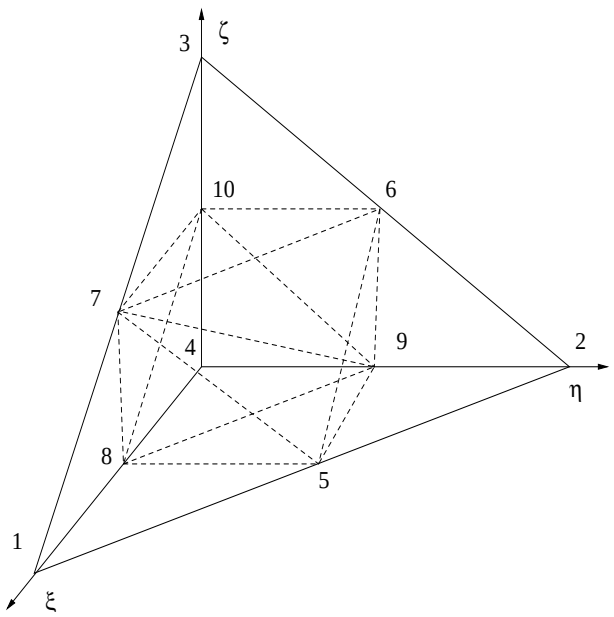

Figure 3: Tetrahedral element in local coordinate system, with axes (ξ,η,ζ)

NUMERICAL RESULTS

- Validation of the scheme: sedimentation problem

$$\frac{\partial \Phi}{\partial t} + \nabla \cdot (\Phi \mathbf{v}) = \mathbf{0} \tag{32}$$

$$\frac{\partial (1-\Phi)}{\partial t} + \nabla \cdot ((1-\Phi)\mathbf{u}) = \mathbf{0} \tag{33}$$

$$\Phi \rho_2 \frac{D_{\mathbf{v}}\mathbf{v}}{\mathbf{Dt}} = -\Phi \nabla p - \xi(\Phi)\nabla\Phi - \beta(\Phi)(\mathbf{v}-\mathbf{u}) + \Phi \rho_{\mathbf{2}}\mathbf{g} -$$

$$\Phi \rho_1 \mu(\Phi) \frac{D_{\mathbf{v}}(\mathbf{v}-\mathbf{u})}{\mathbf{Dt}} \tag{34}$$

$$(1-\Phi)\rho_1 \frac{D_{\mathbf{u}}\mathbf{u}}{\mathbf{Dt}} = -(1-\Phi)\nabla p + \xi(\Phi)\nabla\Phi + \beta(\Phi)(\mathbf{v}-\mathbf{u}) +$$

$$(1-\Phi)\rho_1 \mathbf{g} + \Phi \rho_{\mathbf{1}} \mu(\Phi) \frac{\mathbf{D}_{\mathbf{v}}(\mathbf{v}-\mathbf{u})}{\mathbf{Dt}} \tag{35}$$

NUMERICAL RESULTS cont.

$$\mu(\Phi) = \frac{1}{2}\frac{1+2\Phi}{1-\Phi}$$
$$\beta(\Phi) = c_f((1-\Phi)\rho_1 + \Phi\rho_2)(1-\Phi)\Phi$$
$$g = -\frac{1}{2}\frac{\rho_1+\rho_2}{\rho_1-\rho_2}$$
$$\xi(\Phi, v, u) = \rho_2\xi_1(v_3 - u_3)^2$$
$$c_f = 1 \quad \xi_1 = 1$$

$$\Phi_0[z] = \begin{cases} 0\,, & \text{if } z \in [0, \frac{1}{4}] \\ \frac{1}{2}\left(1 - e^{1-\frac{1}{1-(4(z-\frac{1}{4}))^2}}\right), & \text{if } z \in [\frac{1}{4}, \frac{1}{2}] \\ \frac{1}{2}\,, & \text{if } z \in [\frac{1}{2}, \frac{3}{2}] \\ \frac{1}{2}\left(1 + e^{1-\frac{1}{1-(4(\frac{7}{4}-z))^2}}\right), & \text{if } z \in [\frac{3}{2}, \frac{7}{4}] \\ 1\,, & \text{if } z \in [\frac{7}{4}, 2] \end{cases} \tag{36}$$

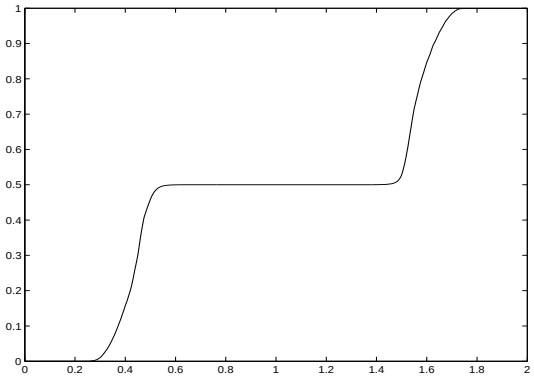

Figure 4: The void fraction profile at iteration=50.

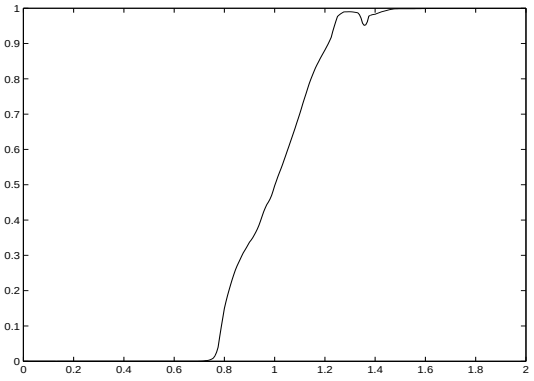

Figure 5: The void fraction profile at iter=1000 (t=1)

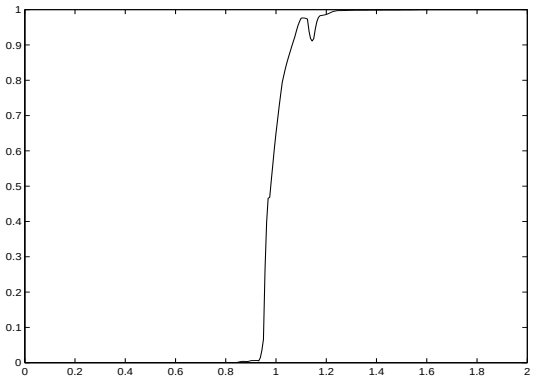

Figure 6: The void fraction profile at iter=1500 (t=1.5)

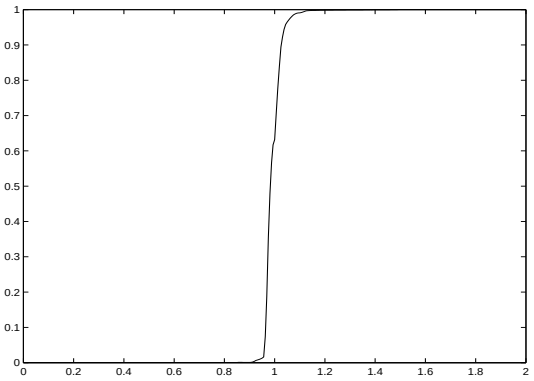

Figure 7: The void fraction profile at iter=2000 (t=2)

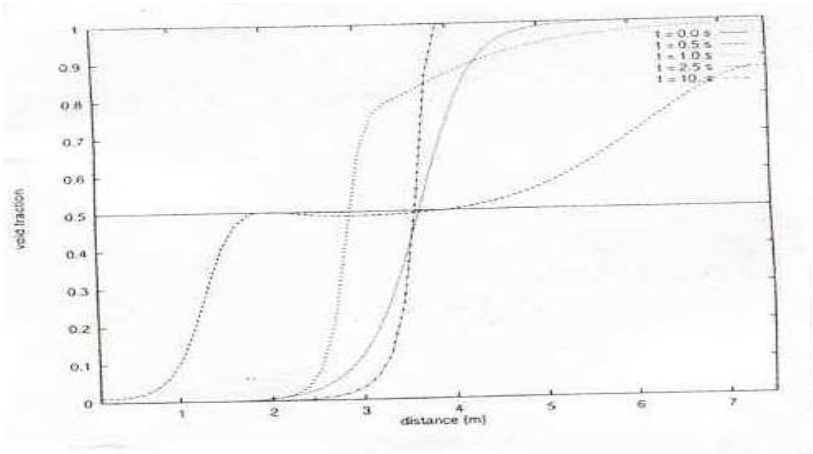

Figure 8: The void fraction profile prescribed by Coquel et al.

NUMERICAL RESULTS(cont.)

- Nonlinear void fraction wave propagation in a real bubble column

  Lammers et al. measured nonlinear long standing waves in the range for the void fraction corresponding to the homogeneous regime. In order for the nonlinear effect to occur in the numerical simulations, we start with an initial nonlinear wave profile given by the signal recorded at the lowest measuring station. The so-called Khokhlov solution is used to fit the measured wave profile.

$$\tilde{\Phi}(\hat{x},\hat{y},\hat{z}=x_1,\hat{t}) = \frac{\hat{t}}{T}\Delta\tilde{\Phi} + \tilde{\Phi}_0 - \frac{1}{2}\Delta\tilde{\Phi} - \frac{1}{2}\,\Delta\tilde{\Phi}\,\tanh(\frac{2}{S}(\hat{z}-\frac{T}{2})),$$

$$\hat{t}\in[0,T]$$

$$\Delta\Phi = 0.05 \quad T = 4.352 \quad S = 1.263.$$

$$\Delta\Phi = 0.05 \quad T = 2.176 \quad S = 0.526.$$

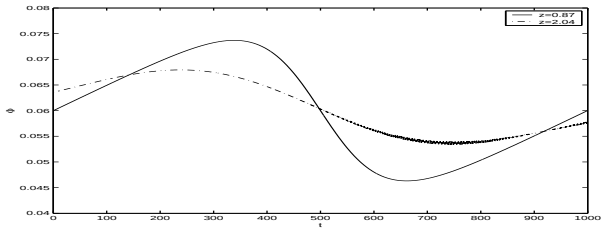

Figure 9: The void fraction profile in the z direction at z=0.87,2.04 when the period T=2.176 $\Phi_0 = 0.06$

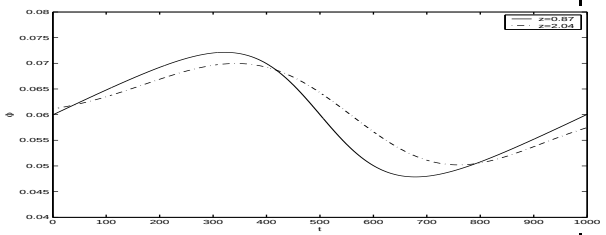

Figure 10: The void fraction profile in the z direction at z=0.87,2.04 when the period T=4.352 $\Phi_0 = 0.06$

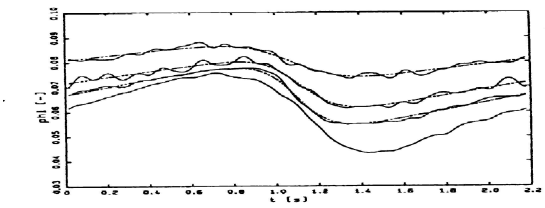

Figure 11: The evolution of sinusoidal finite-amplitude concentration disturbances in time for x=0.87,2.04,3.22,4.47 by Lammers *et al.* (1996) T=2.176 $\Phi_0 = 0.06$

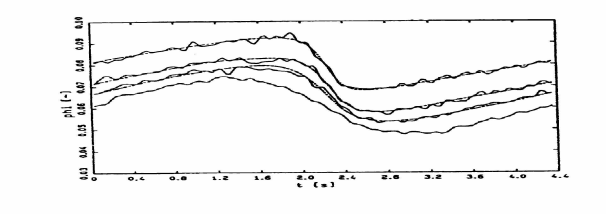

Figure 12: The evolution of sinusoidal finite-amplitude concentration disturbances in time for x=0.87,2.04,3.22,4.47 by Lammers *et al.* (1996) T=4.352 $\lambda = 0.06$ $\Phi_0 = 0.06$

NUMERICAL RESULTS(cont.)

- Growth factor:

  The bubbles increase in size due to the loss of hydrostatic head. That's why we must add mass through the system to the continuity equation for the gas.

  It becomes:

$$\frac{\partial \Phi}{\partial t} + \nabla \cdot (\Phi \mathbf{v}) = \lambda \Phi \mathbf{v} \tag{37}$$

  where

$$\lambda = \frac{\rho_1 g(1 - \Phi_m)}{p_l}$$

$$p_l(z) = P_a + (1 - \Phi_m)\rho_m g(H - z)$$

NUMERICAL RESULTS(cont.)

- Cirulation in gas-liquid column reactors

  We compared our numerical results with the experiments performed by Durst et al.(1984).

  Geometric configuration:
  Diameter=0.1 m
  Height=0.098 m
  Liquid (castor oil): density=960.3 kg/m^3
  kinematic viscosity=0.699*10^{-3} m$^2/s$
  d_b=6 mm.

NUMERICAL RESULTS(cont.)

Boundary Conditions:

- Inlet boundary conditions

$$\Phi[z=0] = \begin{cases} \Phi_0\,, & \text{for } r \in [0, r_s] \\ \\ 0\,, & \text{if } z \in (r_s, R] \end{cases} \tag{38}$$

$$\Phi_0 = 0.12$$

$$\mathbf{u[z=0]=0}$$

$$v_z[z=0] = 0.4 * v_{max}$$

$$v_{max} = 3.09 cm/s$$

- Wall boundary conditions

$$\mathbf{u[r=R]=0}$$

$$v_x[r=R] = 0, v_y[r=R] = 0$$

- Outlet boundary conditions

$$u_z[z=H] = 0$$

$$p[z=H] = 0$$

NUMERICAL RESULTS(cont.)

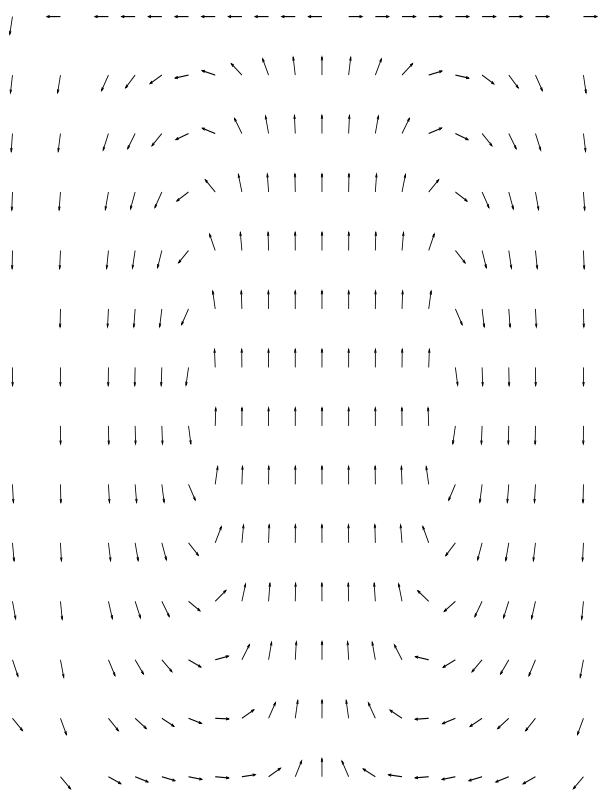

Figure 13: Liquid velocity vector field after the flow reaches the steady state.

NUMERICAL RESULTS(cont.)

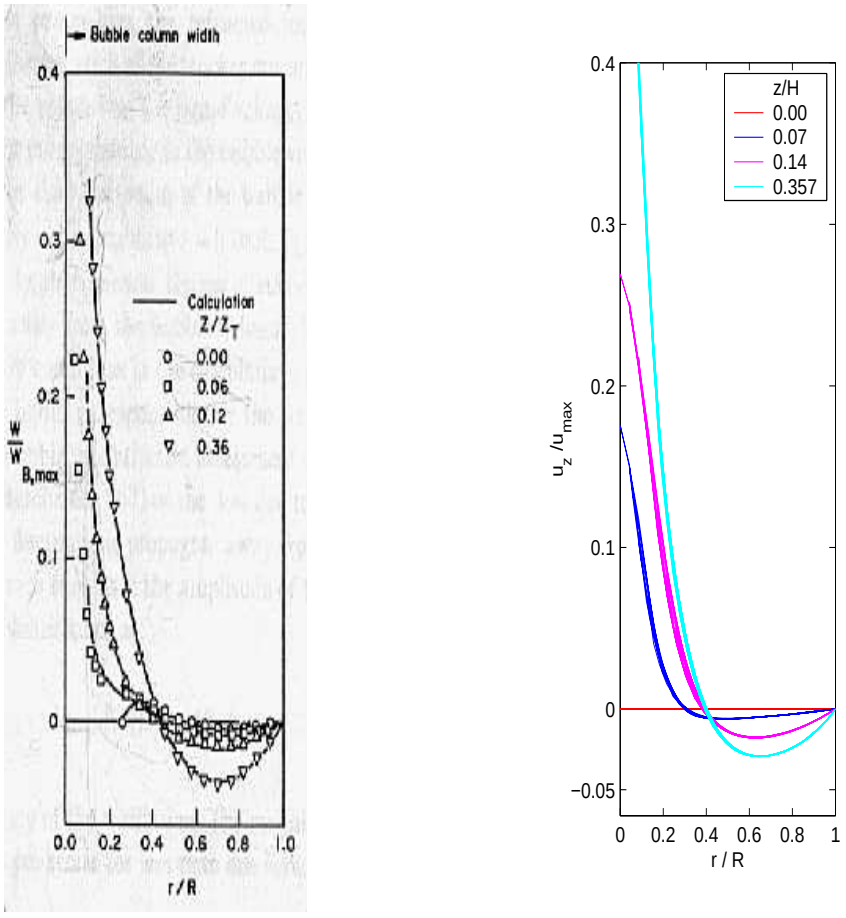

Figure 14: Profiles of the liquid axial velocity at successive axial stations.

NUMERICAL RESULTS(cont.)

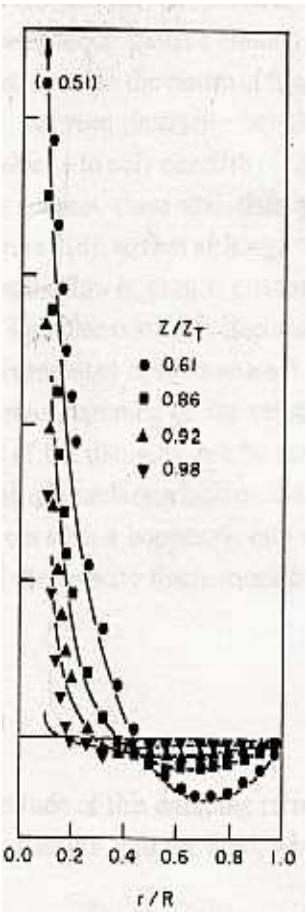

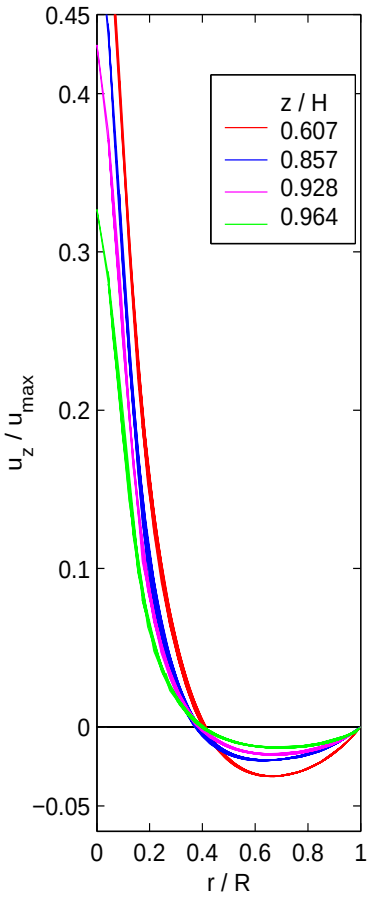

Figure 15: Profiles of the liquid axial velocity at successive axial stations.

REFERENCES

- P. Minev, U. Lange and K. Nandakumar, A comparative study of two-fluid models relevant to bubble column dynamics. **J. Fluid Mech.** 394 (1999), 73-96.
- C. Caia and P. Minev, A finite element method for an averaged multiphase flow model. **Int. J. CFD** 18 (2004), 111-123.

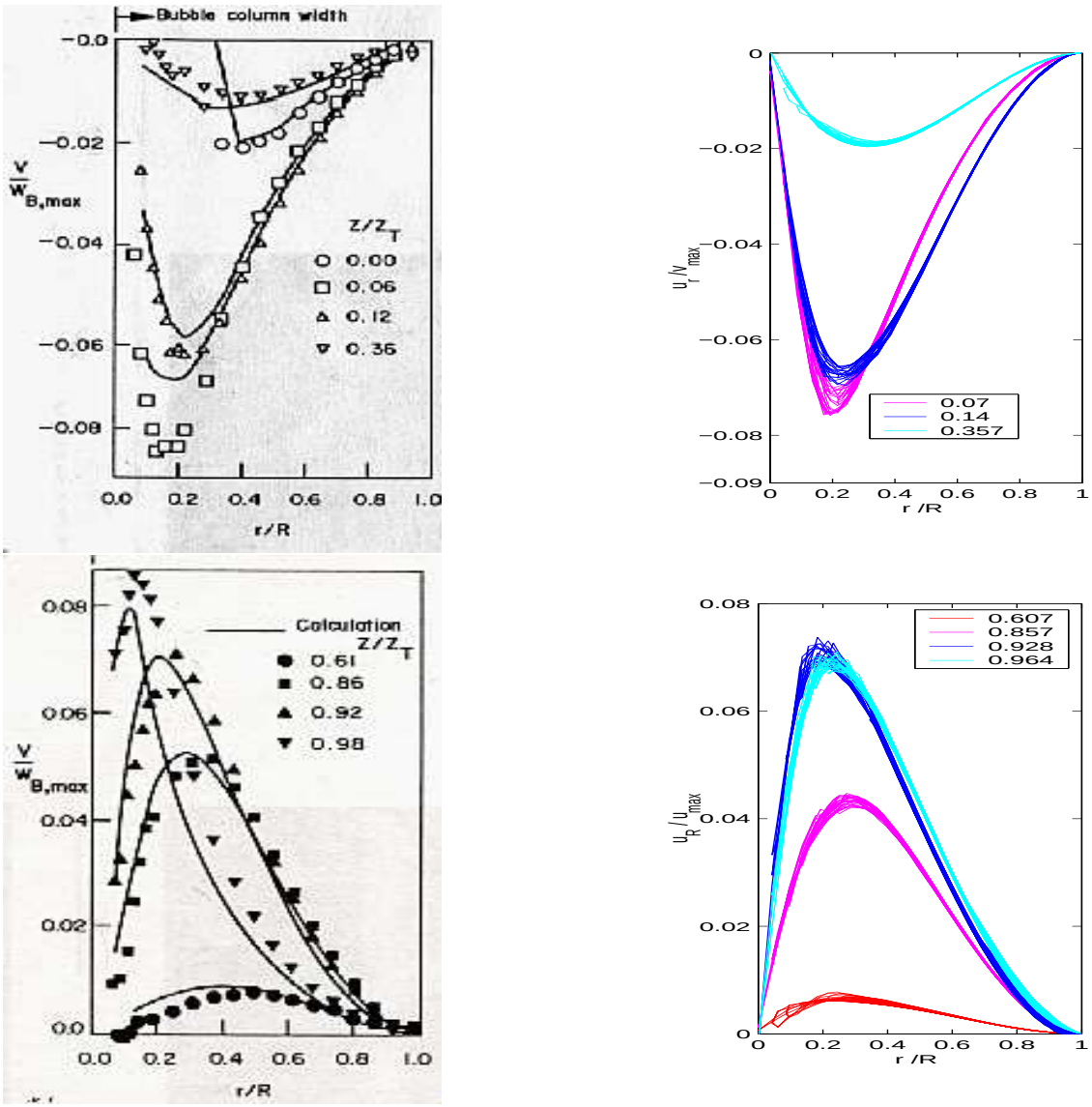

Figure 16: Profiles of the liquid radial velocity at successive axial stations.

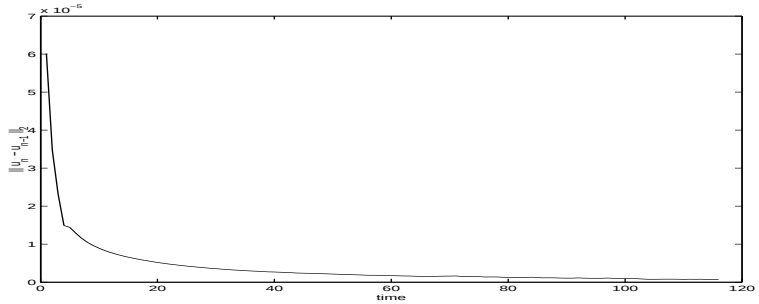

Figure 17: The liquid velocity reaches steady state

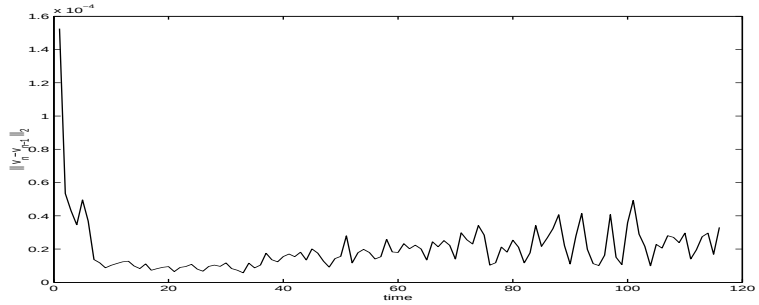

Figure 18: The gas velocity reaches steady state

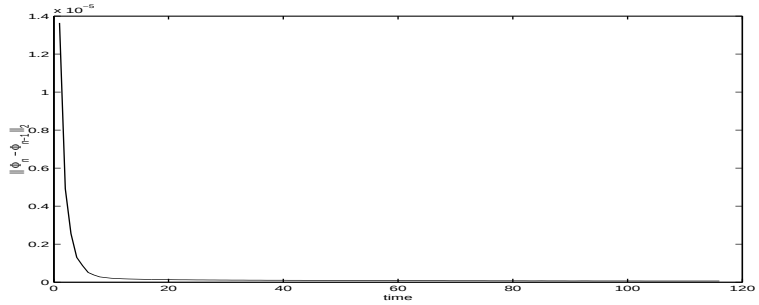

Figure 19: The void fraction reaches steady state